J. Biochem. 2010;148(4):449–458 doi:10.1093/jb/mvq079

JB THE JOURNAL OF BIOCHEMISTRY

Remarkable improvement in the heat stability of CutA1 from *Escherichia coli* by rational protein design

Received June 13, 2010; accepted July 6, 2010; published online July 16, 2010

Yoshinori Matsuura[1], Motonori Ota[2], Tomoyuki Tanaka[1], Michiyo Takehira[1], Kyoko Ogasahara[3], Bagautdin Bagautdinov[1], Naoki Kunishima[1] and Katsuhide Yutani[1,*]

[1]RIKEN SPring-8 Center, Harima Institute, RIKEN; 1-1-1 Kouto, Sayo, Hyogo 679-5148; [2]Graduate School of Information Science, Nagoya University; Furo-cho, Chikusa-ku, Nagoya 464-8601; and [3]Institute for Protein Research, Osaka University; 3-2 Yamada-oka, Suita, Osaka, 565-0871, Japan

*Katsuhide Yutani, RIKEN SPring-8 Center, Harima Institute, 1-1-1 Kouto, Sayo, Hyogo 679-5148, Japan. Tel: +81 791 58 2937, Fax: +81 791 58 2917, email: yutani@spring8.or.jp

To enhance the heat stability of the CutA1 protein from *Escherichia coli* (*Ec*CutA1) so that it has comparable stability to CutA1 from *Pyrococcus horikoshii* with a denaturation temperature (T_d) of 150°C, we used the Stability Profile of Mutant Protein (SPMP) to examine the structure-sequence (3D-1D) compatibility between the conformation of *Ec*CutA1 and its native sequence [*J. Mol. Biol.*, 248, 733-738, (1995)]. We identified seven residues in *Ec*CutA1 that were incompatible in terms of dihedral angles and hydrophobicity. These residues were replaced with appropriate amino acids, and the mutant proteins were evaluated for changes in stability by DSC and denaturant denaturation. The mutations that were introduced at five out of the seven positions improved the stability of *Ec*CutA1. The T_d values of single (S11A) and triple (S11V/E61V/Q73V) mutants improved by 16.5 and 26.6°C, respectively, compared to that of the wild-type protein (89.9°C). These analyses showed that (1) the stability of *Ec*CutA1 is remarkably improved by slight substitutions, even though the stability of the wild-type protein is considerably high, (2) remarkable improvements in the stability can be quantitatively explained based on the newly solved native structure, and (3) SPMP is a powerful tool to examine substitutions that improve protein stability.

Keywords: CutA1/design of protein stabilization/protein denaturation/protein stability/protein structure.

Abbreviations: *Ec*CutA1, CutA1 protein from *Escherichia coli*; *Ph*CutA1, CutA1 from hyperthermophile, *Pyrococcus horikoshii*; *Tt*CutA1, CutA1 from an extreme thermophile, *Thermus thermophilus*; SPMP, Stability Profile of Mutant Protein; T_d, denaturation temperature.

Globular proteins generally have a low conformational stability of ~50 kJ/mol, which is balanced by a combination of many stabilizing and destabilizing factors (interactions) such as hydrophobic interactions, hydrogen bonds, electrostatic interactions, and entropic effects (*1*, *2*). Although the magnitude of each factor is not small (5–25 kJ/mol), these positive and negative factors compensate each other, resulting in marginal stability. Studies on mutant proteins can estimate the effects of various stabilizing factors. Extensive studies on stabilization mechanisms have been conducted using mutant proteins (*3*–*9*) and hyperthermophile proteins (*10*–*15*). However, substitutions with the same types of amino acids have often given different results and the effects of these changes on protein stability differ depending on the surrounding environment, substituted residues, and structural changes due to the mutations (*3*, *4*). There are no established methods that can be used to rationally design an enhanced conformational stability, and it is important to develop these techniques because stability-enhanced proteins may be highly useful for industrial and biotechnological processes (*16*).

Recently, we found that the CutA1 protein from *Pyrococcus horikoshii* (*Ph*CutA1) has an unusually high stability at a neutral pH with a denaturation temperature (T_d) near 150°C, which is ~30°C greater than the highest value determined by differential scanning calorimetry (DSC) (*15*). The CutA1 protein was originally identified in the *cutA* gene locus of *Escherichia coli*, which is involved in divalent metal tolerance. The X-ray crystal structures of CutA1 from various species have been solved and the common trimer structures are highly similar across these species. A structural analysis of both *Ph*CutA1 and *E. coli* CutA1 (*Ec*CutA1) revealed that the remarkably increased number of ion pairs, hydrogen bonds and hydrophobic interactions in the monomer contributes to the stabilization of the *Ph*CutA1 trimer (*15*). On the other hand, the T_d of *Ec*CutA1 was 89.9°C at pH 9, which is also significantly higher than other proteins from the mesophile *E. coli*. CutA1 proteins from rice (*Oryza sativa*) and humans (*Homo sapiens*, brain) also have high T_d values of 97.3 and 96.2°C at pH 7.0, respectively (*17*). In order to determine the key elements that improve the T_d, we used protein engineering to enhance the heat stability of *Ec*CutA1 so that it has a T_d that is comparable to the T_d of 150°C for *Ph*CutA1. The reverse strategy, in which the unstable mutants are created from *Ph*CutA1, is not promising because it is likely

that every mutation will destabilize the protein, making it difficult to identify the essential residues for stabilization. Therefore, creating a protein with a $T_d = 150°C$ from *Ec*CutA1 is a better approach to confirm the thermo-stabilization mechanism of *Ph*CutA1 and to establish a method to rationally improve the conformational stability of a protein.

As a first step in the mutation strategy to enhance the heat stability of the CutA1 protein from *Ec*CutA1, we examined the structure-sequence (3D-1D) compatibility between the conformation of *Ec*CutA1 and its native sequence using Stability Profile of Mutant Protein (SPMP). SPMP estimates changes in the stability of 19 mutant proteins at every position of a protein based on the X-ray crystal structure (*18–20*). We chose seven incompatible positions in *Ec*CutA1, which were predicted from SPMP, and then introduced single and multiple point mutations at these locations. The stabilities of the constructed *Ec*CutA1 mutants were evaluated by heat and denaturant denaturation, and their structures were determined by X-ray crystallography. We will discuss the stabilization mechanism of the mutant proteins based on the X-ray crystalline structure and 3D-1D compatibility.

Experimental Procedures

Cloning, expression and purification of CutA1 from E. coli

The *Ec*CutA1 gene was polymerase chain reaction (PCR) amplified using *PfuTurbo* DNA polymerase (Stratagene) and *E. coli* K-12 W3110 genomic DNA. The primers used to amplify *Ec*CutA1 gene were 5′-GATATACATATGCTTGATGAAAAAAGTTCG-3′ and 5′-AAAGGATCCTCAGCGTAAAGATGCGTTGAGC-3′. The full-length PCR products were digested with *Nde*I and *Bam*HI, and the fragment was inserted into the pET-11a expression vector (Novagen) that had been linearized with *Nde*I and *Bam*HI. All of the prepared mutants using the *Ec*CutA1 gene were generated using a QuikChange II XL site-directed mutagenesis kit (Stratagene). The sequence was confirmed by DNA sequencing.

For protein production, *E. coli* BL21-CodonPlus(DE3)-RIL competent cells were transformed with the recombinant plasmid and grown at 37°C in Luria–Bertani medium containing 50 μg/ml ampicillin for 20 h. The cells were harvested by centrifuging at 4,500*g* for 5 min at 4°C, suspended in 20 mM Tris–HCl, pH 8.0, containing 0.5 M NaCl and 2 mM EDTA, and finally disrupted by sonicating and heating at 70–90°C for 15 min. The cell debris and heat-denatured proteins were removed by centrifuging at 20,000*g* for 30 min. The supernatant was used as the crude extract for purification.

The crude extract was desalted on a HiPrep 26/10 desalting column (GE Healthcare) and applied to a Super Q Toyopearl 650 M (Tosoh) column equilibrated with 20 mM Tris–HCl, pH 8.0, containing 2 mM EDTA (buffer A). After eluting with a linear gradient of 0.2–1.4 M NaCl, the fractions containing *Ec*CutA1 were collected. Ammonium sulphate was added to the sample to a final concentration of 1.5 M, and the soluble fraction then applied to a Resource PHE column (GE Healthcare) equilibrated with 50 mM sodium phosphate buffer, pH 7.0, containing 1.5 M ammonium sulphate and 2 mM EDTA. The *Ec*CutA1-containing fractions were eluted with a linear gradient of 0.75–0 M ammonium sulphate. The sample was concentrated by ultrafiltration (VivaSpin, 5 kDa cut-off) and loaded onto a HiLoad 16/60 Superdex 75 prep-grade column (GE Healthcare) equilibrated with buffer A containing 0.2 M NaCl. The homogeneity and identity of the purified sample were assessed by SDS–PAGE. The concentrations of the wild-type and mutant proteins were estimated from the absorbance at 280 nm, assuming $E^{1cm}_{1\%} = 14.96$, which is based on the number of aromatic amino acids (*21*).

DSC experiments

DSC was performed at scan rate of 60°C/h using a VP-capillary DSC platform. For the measurements, the protein concentrations were 0.25–0.68 mg/ml in 50 mM glycine buffer at pH 9.0 containing 2 mM EDTA and 5 mM β-mercaptoethanol. All samples were dialysed against the buffers overnight at 4°C and then filtered through a 0.22-μm pore size membrane. The denaturation temperature (T_d) represents the peak temperature of the DSC curves. The T_d values in this study represent the average of at least six experiments.

Guanidine hydrochloride-induced unfolding and refolding

For the denaturant unfolding experiment, the wild-type and mutant *Ec*CutA1 were incubated in various guanidine hydrochloride (GuHCl) concentrations at pH 8.0 and 37°C for various time frames. For the refolding experiment, the proteins were completely unfolded in the presence of 7 M GuHCl for 15 min at 95°C and then diluted with 20 mM Tris–HCl buffer at pH 8.0 containing 0.2 mM EDTA, 0.1 mM DTE (dithioerythritol), and various concentrations of GuHCl at 37°C. The unfolding and refolding reactions were monitored by measuring the CD values at 220 nm. The CD measurements were carried out using a Jasco J-725 spectropolarimeter. The unfolded fraction was calculated using equation (*1*) reported in our previous paper (*17*). The refolding curves were analysed by a linear extrapolation model assuming a two-state transition for the unfolding of a trimer protein, according to the following equations (*17*, *22*).

$$N_3 \leftrightarrow 3U \tag{1}$$

$$K = 27Ct^2 f_u^3/(1 - fu) \tag{2}$$

$$\Delta G^0 = -RT \ln K \tag{3}$$

$$\Delta G^0 = \Delta G^0_{H_2O} + m[x] \tag{4}$$

$$\begin{aligned} f_u = & (((1/2)((exp(-(\Delta G^0_{H_2O}+mx)/(RT)))/(27Ct\hat{}2))+(1/18) \\ & ((exp(-(\Delta G^0_{H_2O}+mx)/(RT)))/(27Ct\hat{}2))(4((exp(-(\Delta G^0_{H_2O}+mx) \\ & /(RT)))/(27Ct\hat{}2))+27)\hat{}(1/2)3\hat{}(1/2))\hat{}(1/3) \\ & -(1/3)((exp(-(\Delta G^0_{H_2O}+mx)/(RT)))/(27Ct\hat{}2))/((1/2) \\ & ((exp(-(\Delta G^0_{H_2O}+mx)/(RT)))/(27Ct\hat{}2))+(1/18) \\ & ((exp(-(\Delta G^0_{H_2O}+mx)/(RT)))/(27Ct\hat{}2)) \\ & (4((exp(-(\Delta G^0_{H_2O}+mx)/(RT)))/ \\ & (27Ct\hat{}2))+27)\hat{}(1/2)3\hat{}(1/2))\hat{}(1/3)) \end{aligned} \tag{5}$$

where K, Ct and ΔG^0 are the equilibrium constant of the unfolding reaction, the molar concentration of the protein expressed in trimer equivalents, and the Gibbs energy change upon unfolding (standard value), respectively. Factor m is the slope of the linear correlation between ΔG^0 and the GuHCl concentration (x). Factor f_u in equation (*5*) is represented as a function of the GuHCl concentration. We used the data analysis software in MicroCal Origin (Northampton, MA, USA) to produce a least squares fit of the experimental data in the GuHCl unfolding curves to obtain $\Delta G^0_{H_2O}$, where $\Delta G^0_{H_2O}$ is the standard value (in 1M protein concentration) in the absence of GuHCl (in water).

Crystallization and X-ray data collection

A 1.5-μl aliquot of S11V (23 mg/ml), E61V (21 mg/ml) and S11V/E61V (19 mg/ml) in 20 mM Tris buffer at pH 8.0 including 0.2 M NaCl and 2 mM EDTA was mixed with an equal volume of reservoirs A, B and C, respectively. Reservoir A contains ~76% of the Crystal Screen 1 (no. 38) from Hampton Research which comprises to 0.1 M HEPES-NaOH (pH 7.5) and 1.4 M tri-sodium citrate. Reservoirs B and C contain ~80% of the SaltRx no. 22 and 21 from Hampton Research, respectively, which comprises 1.2 M tri-sodium citrate containing 0.1 M Tris (pH 8.5) and 0.1 M Bis-Tris propane (pH 7.0), respectively. Crystals suitable for data collection were obtained using the hanging-drop vapour diffusion method over several days at 20°C. X-ray diffraction data for S11V and S11V/E61V were

collected at the RIKEN structural genomics beamline BL26B2 of SPring-8, and data for E61V were collected using an in-house R-axis VII system (Rigaku).

Structure solution and refinement

The structures of S11V, E61V and S11V/E61V were determined by the molecular replacement method using the wild-type CutA1 from *E. coli* (PDB code, 1NAQ) as the search model. The solution was determined by using automated-MOLREP within the CCP4 program suite (*23*), and then refined using CNS (*24*). The protein model was built using Coot (*25*). The quality of the models was inspected by Procheck (*26*). The quality of both structural residues in the most favoured regions was over 90%, and there were no residues in the generously allowed or disallowed regions. The statistics for the data collection and refinement are summarized in Table I.

Calculation of changes in unfolding Gibbs energy due to the hydrophobic interaction

To estimate the difference ($\Delta\Delta G_{HP}$) in the unfolding Gibbs energy (ΔG) between the wild-type and mutant proteins due to hydrophobic interactions, the following equation is proposed using structural information such as *ASA* (accessible surface area) (*4*).

$$\Delta\Delta G_{HP} = 0.146\Delta\Delta ASA_{non-polar} + 0.021\Delta\Delta ASA_{polar} \quad (6)$$

where $\Delta\Delta ASA_{non\text{-}polar}$ and $\Delta\Delta ASA_{polar}$ represent the differences in the ΔASA of the non-polar and polar atoms of all residues, respectively, between the wild-type and the mutant proteins upon denaturation. The parameters of equation (*6*) have been obtained using the stability/structure database upon the denaturation of mutant human lysozymes and T4 lysozyme. To calculate the *ASA* value, the carbon and sulphur atoms in the residues are assigned to $ASA_{non\text{-}polar}$, and the nitrogen and oxygen atoms are represented by ASA_{polar}. The *ASA* values of the native state were calculated following the procedure proposed by Connolly (*27*), using the X-ray crystal structures of the mutant CutA1 proteins. The *ASA* values for the denatured forms were estimated using the extended structures of each protein, which were generated from the native structures using the programme Insight II.

Results and Discussion

*Ec*CutA1 mutants

Ota *et al.* (*20*) proposed that changes in the stability of 19 mutant proteins at every position in a protein can be estimated by knowledge-based potential if the X-ray crystal structure data are available. This method is called SPMP analysis, and we used SPMP to examine the structure-sequence (3D-1D) compatibility of *Ec*CutA1. A pseudo-energy potential (ΔG_{SPMP}) derived from a number of PDB structures is used in SPMP. This potential was originally developed to predict protein structures and consists of four elements, *i.e.* the side-chain packing (ΔG_{SP}), hydration (ΔG_{Hyd}), local structure (ΔG_{LC}) and back-bone-side-chain repulsion (ΔG_{BR}) as expressed by the following equation.

$$\Delta G_{SPMP} = \Delta G_{SP} + \Delta G_{Hyd} + \Delta G_{LC} + \Delta G_{BR} \quad (7)$$

Table II shows the SPMP scores of the native amino acids in the chain A of trimer *Ec*CutA1 (PDB code: 1NAQ) for the four SPMP elements in order of worst (the most incompatible amino acid) to best. The 'rank' column in Table II shows the rank position of the wild-type amino acid at the specified position out of 20 amino acids, and the 'fitness of amino acid' column lists the 20 amino acids from the most compatible to the worst. The most incompatible amino acid estimated by SPMP was Lys67, but Lys67 and Glu90 form a salt bridge in the wild-type structure. Generally, the estimation of electrostatic interaction is known to be difficult for the knowledge-based potentials, as was employed by SPMP. Then, we considered that Lys67 would not necessarily be incompatible. The rank positions of the wild-type amino acids

Table I. Data collection and refinement statistics of mutant CutA1 proteins from *E. coli*.

	S11 V	E61 V	S11 V/E61 V
Data collection			
Wavelength (Å)	1.000	1.54178	1.000
Space group	$P2_12_12_1$	$P2_12_12_1$	$P6_1$
Cell dimension (Å)	$a = 62.239$	$a = 38.187$	$a = b = 52.664$
	$b = 96.872$	$b = 50.101$	$c = 178.361$
	$c = 106.352$	$c = 147.424$	
No. of molecule/asu	6	3	3
Resolution range (Å)	40.0–2.40 (2.49–2.40)	40.0–2.30 (2.38–2.30)	40.0–2.30 (2.38–2.30)
Unique reflections	25,891	13,267	12,446
Redundancy	7.0 (7.0)	6.4 (6.1)	9.6 (6.2)
Completeness (%)	100	99.4	99.6
R_{merge} (%)	6.2 (30.0)	3.5 (10.5)	11.7 (33.0)
Refinement statistics			
Resolution range (Å)	40–2.4	40–2.3	40–2.3
Reflection used in refinement	25,793	13,222	12,336
R_{work}	0.202	0.205	0.174
R_{free}	0.251	0.247	0.238
No. of water molecules	226	114	300
RMSD bond length (Å)	0.0062	0.0059	0.0057
RMSD bond length (angle)	1.203	1.151	1.135
Ramachandran statistics			
Most favoured region (%)	93.6	92.5	94.0
Additional allowed region (%)	6.4	7.5	6.0
PDB code	3AH6	3AA9	3AA8

Values in parentheses refer to the highest resolution shell.

listed in Table II were very low and they were ranked worse than 12th, except for Val96, which was ranked 9th (see the rank column in Table II). Therefore, seven positions except for these three residues at positions 67, 90 and 96 were mutated to improve the protein stability. The bold and bold-underlined letters in the fitness column of amino acids in Table II show the wild-type and substituted residues, respectively. Single and multiple mutations were constructed at these sites, which are highlighted in the crystal structures of wild-type *Ec*CutA1 in Fig. 1. The first rank amino acid at position 45, 61 and 73 in Table II was not chosen because the side-chains are more bulky than that of the wild-type residues. The SPMP was also applied to evaluate mutations based on *Ec*CutA1 mutant structures determined in this study (Table III, described later).

DSC experiments on mutant EcCutA1

To measure the changes in stability due to the mutations, DSC experiments were conducted with the mutant proteins at pH 9.0. Typical DSC curves for the wild-type and mutant proteins are shown in Fig. 2, and the T_d of the wild-type and all of the mutant proteins are listed in Table IV. The T_d values were obtained from the peak temperature of the DSC curves because heat denaturation is not reversible. The stability of the constructed *Ec*CutA1 mutants was

Table II. SPMP scores of *Ec*CutA1 for the four elements, in the order of worst to best.

Order	Position	Wild-type	SS[a]	Burial[b]	ΔG_{SPMP}	ΔG_{SP}	ΔG_{Hyd}	ΔG_{LC}	ΔG_{BR}	Rank[c]	Fitness of amino acids[d]
1	67	Lys	E	8	2.63	−1.21	2.26	1.30	0.29	17	FIYVLCMWHTSAGQRN**K**PDE
2	11	Ser	E	9	1.76	−0.42	1.09	1.00	0.08	13	**V**C**IA**MLYFTPWH**S**GQNERDK
3	73	Gln	H	6	1.42	1.59	0.25	−0.75	0.33	14	I**V**MLCTFSHAWYG**Q**KERNDP
4	59	Glu	E	5	1.25	−0.50	−0.04	1.71	0.08	15	**L**HFWYCRMVIT**QK**S**E**PNADG
5	45	Gly	E	5	1.21	0.21	0.00	1.00	0.00	19	MLVTIC**Q**YWSFHREPAKN**G**D
6	86	Tyr	C	2	0.96	0.00	2.01	−1.05	0.00	12	**D**NTSEKQRHCA**Y**WMIFGLVP
7	60	Tyr	E	2	0.92	−0.67	2.47	−0.96	0.08	13	**T**ESQKRHNGVPD**Y**MFIALWC
8	61	Glu	E	6	0.88	−1.76	0.63	1.71	0.29	12	W**THV**YCFSAIN**E**QRPDGMLK
9	96	Val	C	6	0.88	−0.67	−0.13	1.46	0.21	9	CSTGNADP**V**HMEWIQLYFRK
10	90	Glu	C	6	0.75	−0.71	0.71	0.59	0.17	18	PRWYFHGACKQVTSIMN**E**LD

ΔG_{SPMP}, ΔG_{SP}, ΔG_{Hyd}, ΔG_{LC} and ΔG_{BR} represent scores of the wild-type amino acid, side-chain packing, hydration, local structure, and back-bone-side-chain repulsion, respectively. Negative values of ΔG means 'stabilization'. The unit is kJ/mol of a monomer.
[a]SS: secondary structure determined by DSSP (*30*). Structures other than α helix (H) and β strand (E) are denoted as coil (C).
[b]Burial: degree of residue burial of the site (1: exposed to water, 9: buried in the protein)
[c]Rank: fitness rank position of the wild-type amino acid at the position out of 20 amino acids
[d]Fitness of amino acids: 20 amino acids sorted from the most compatible one to the most incompatible one. Bold and bold-underlined letters denote the wild-type and substituted residues in this study, respectively.

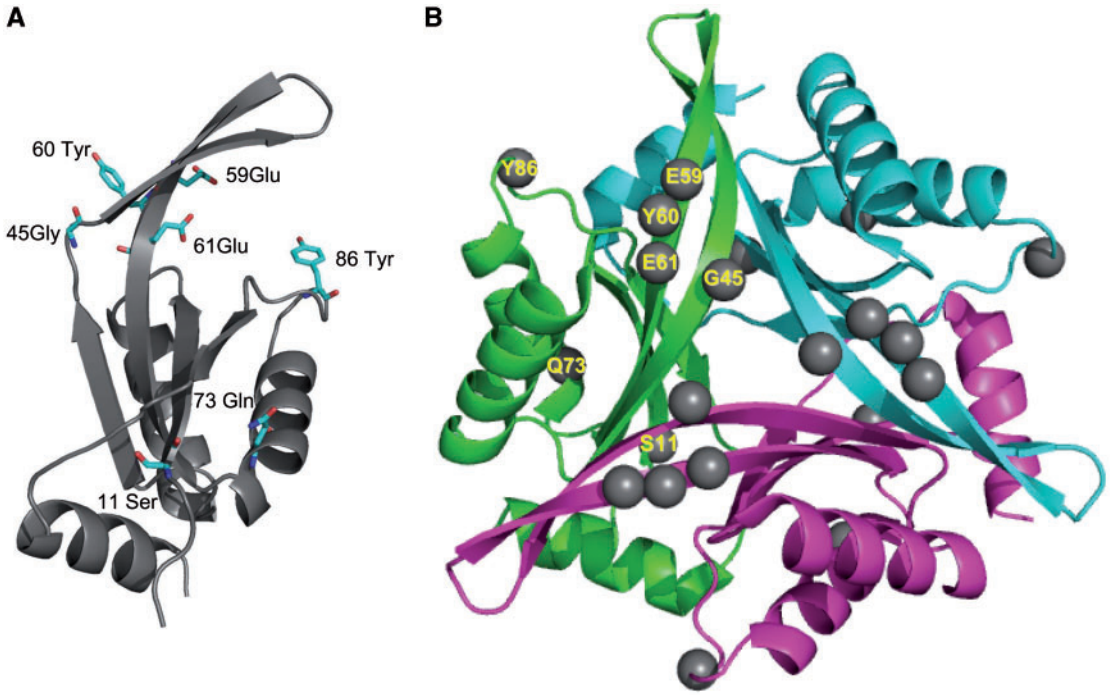

Fig. 1 The crystal structure of the wild-type *Ec*CutA1. (A) Monomer structure of the wild-type *Ec*CutA1 (1NAQ). The labeled names represent the substituted residues**.** (B) Trimer structure of the wild-type *Ec*CutA1 (1NAQ). The different colours represent the different subunits. Black circles denote the substituted residues.

Table III. SPMP evaluation at the mutation sites of the three solved mutant structures and the wild-type one.

Proteins	Position	ΔG_{SPMP}	ΔG_{SP}	ΔG_{Hyd}	ΔG_{LC}	ΔG_{BR}	Rank
S11 V	11Val	−6.16 ± 0.55	−3.23	−1.53	−1.49	0.10	1
	61Glu	0.91 ± 0.48	−2.03	0.63	1.71	0.59	15
E61 V	11Ser	1.21 ± 0.04	−0.18	0.99	0.32	0.08	12
	61Var	−2.09 ± 0.08	−1.24	−0.24	−1.30	0.68	7
S11 V/E61 V	11Val	−5.57 ± 0.79	−2.58	−1.55	−1.50	0.06	1
	61Val	−1.02 ± 0.92	−0.06	−0.15	−1.30	0.49	7
Wild-type	11Ser	1.76	−0.42	1.09	1.00	0.08	13
	61Glu	0.88	−1.76	0.63	1.71	0.29	12

The total SPMP values for E61 V and S11 V/E61 V show average of three subunits and its deviation. Those of S11 V are the average of 6 subunits in an asymmetric unit. Negative values of ΔG mean 'stabilization'. The values of the four elements show only average values of three subunits.

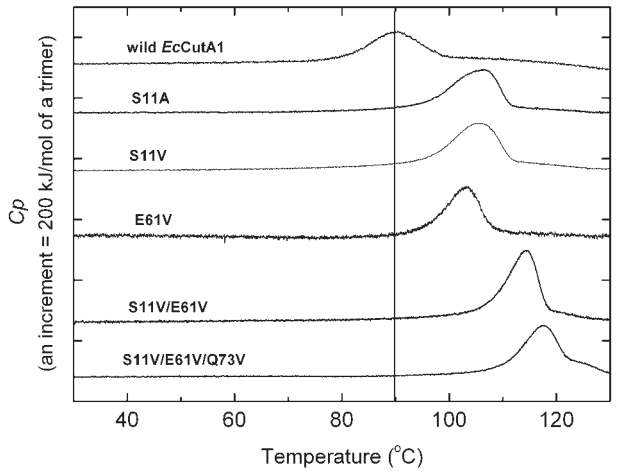

Fig. 2 Typical DSC curves of the wild-type and mutant *Ec*CutA1 at pH 9.0. The scan rate of each DSC curve was 60°C/h. The perpendicular line at 89.9°C shows the T_d value of the wild-type protein.

improved at five out of the chosen seven positions. The T_d values for S11A, E59K, Y60T, E61V and Q73V were 106.4, 104.2, 91.9, 103.4 and 94.0°C at pH 9.0, respectively. S11A was improved by 16.5°C compared to the wild-type (89.9°C), whereas G45Q (82.1°C) and Y86D (76.8°C) were lower. Multiple mutants at the improved positions were also constructed; the T_d values of S11V/E61T, S11V/E61V and S11V/E61V/Q73V were 112.3, 113.5 and 116.5°C, respectively. The highest one was improved by 26.6°C. These results indicate that the stability of *Ec*CutA1 is remarkably improved by single and multiple substitutions, even though the T_d of the wild-type protein is considerably high, near 90°C.

Denaturant denaturation of mutant EcCutA1

DSC experiments showed only the apparent denaturation temperatures of all of the mutant proteins because the heat denaturation process was irreversible. Therefore, in order to evaluate the thermodynamic parameters of denaturation, the unfolding and refolding curves for the wild-type and mutant proteins were analysed using the denaturant guanidine hydrochloride (GuHCl). The unfolding curves for all of the proteins versus the various GuHCl concentrations did not reach a constant value even after several days, indicating that the GuHCl-induced denaturation rate is remarkably slow and similar to that for CutA1 proteins from other sources (*17*). However, the refolding curves for the wild-type and mutant proteins were highly similar after 1- and 2-day incubations at 37°C, suggesting that the refolding reaction reached equilibrium after a 1-day incubation at 37°C. Figure 3 shows the typical refolding curves for the wild-type and mutant proteins after 1 day at pH 8.0 and 37°C. These refolding curves were analysed using the linear extrapolation model assuming a two-state transition for the unfolding of a trimer protein ($N_3 \leftrightarrow 3U$) using equation (*5*). The solid curves in Fig. 3 represent the fitting lines using equation (*5*). The unfolding thermodynamic parameters that were obtained from the GuHCl refolding curves for the examined proteins are listed in Table IV. The midpoint of the S11V/E61V/Q73V refolding curve was 4.67 M GuHCl, which is remarkably higher than that of the wild-type protein (2.72 M). The $\Delta G^0_{H_2O}$ of S11V/E61V/Q73V was 258.9 kJ/mol (Table IV). These thermodynamic parameters were higher than the T_d (112.8°C), $\Delta G^0_{H_2O}$ (207.7 kJ/mol), and midpoint (3.33 M) of CutA1 (*Tt*CutA1) from an extreme thermophile, *Thermus thermophilus*, which grows at approximately 75°C (*17*). The thermodynamic parameters of the double mutant S11V/E61V were also higher than those of *Tt*CutA1. These results indicate that substitutions at only two positions in the mesophile protein greatly improve the protein stability to a level that exceeds the stability of an extreme thermophile protein.

The relationship between the thermodynamic parameters from the GuHCl denaturation and the T_d from the DSC experiments were examined as shown in Fig. 4. There was a good correlation between $\Delta G^0_{H_2O}$ and T_d with a correlation coefficient of 0.86 (Fig. 4). Overall, these results indicate that changes in the heat stability of these mutants roughly parallel those for the denaturant denaturation at 37°C.

Crystal structures of mutant CutA1 and SPMP evaluations

The stabilities of the proteins with mutations at positions 11 and 61 were remarkably improved as shown in Table IV. Therefore, the tertiary structures of three mutant proteins, S11V, E61V and S11V/E61V, were determined by X-ray crystallography to confirm the structural changes due to these mutations. The overall

Table IV. Thermodynamic parameters of unfolding for the wild-type and mutant *Ec*CutA1 proteins.

Proteins	*Td* (°C)*	$\Delta G^0_{H_2O}$ (kJ/mol)*	Midpoint (M)*	*m* (slope) (kJ/mol M)*	$\Delta\Delta G^0_{H_2O}$ (kJ/mol)**
Wild-type	89.9 ± 0.5	165.2 ± 10.2	2.72 ± 0.01	−35.2 ± 2.1	0
S11 V	105.0 ± 0.8	205.9 ± 8.8	3.31 ± 0.00	−41.2 ± 1.3	40.7
S11 A	106.4 ± 0.2	185.9 ± 8.1	3.06 ± 0.00	−38.3 ± 1.2	20.7
S11I	102.7 ± 0.8	ND	ND	ND	
G45Q	82.1 ± 1.2	ND	ND	ND	
E59 L	100.2 ± 0.3	177.3 ± 10.9	2.96 ± 0.01	−36.1 ± 2.7	12.1
E59 K	104.2 ± 0.1	181.6 ± 9.5	3.01 ± 0.01	−37.2 ± 1.9	16.4
E59Q	98.3 ±0.7	ND	ND	ND	
Y60 T	91.9 ± 2.1	ND	ND	ND	
E61 V	103.4 ± 0.4	179.5 ± 9.5	3.29 ± 0.01	−33.3 ± 1.5	14.3
E61 T	98.6 ± 0.2	178.4 ± 10.0	2.99 ± 0.01	−34.5 ± 1.2	13.2
E61 H	94.3 ± 1.7	ND	ND	ND	
Q73 V	94.0 ± 2.3	147.9 ± 7.3	3.40 ± 0.02	−23.0 ± 1.4	−17.3
Y86D	76.8 ± 0.1	138.5 ± 2.6	2.67 ± 0.01	−25.9 ± 0.7	−26.7
S11 V/E61 T	112.3 ± 0.1	201.3 ± 17.3	3.48 ± 0.01	−34.7 ± 1.7	36.1
S11 V/E61 V	113.5 ± 0.4	245.0 ± 20.1	3.80 ± 0.01	−44.7 ± 2.0	79.8
E59 K/E61 V	104.3 ± 0.3	188.1 ± 19.2	3.24 ± 0.01	−36.6 ± 2.8	22.9
S11 V/E61 T/Q73 V	113.6 ± 0.6	202.4 ± 15.2	4.20 ± 0.01	−30.0 ± 1.4	37.2
S11 V/E61 V/Q73 V	116.5 ± 0.7	258.9 ± 42.2	4.67 ± 0.01	−34.8 ± 2.5	93.7
S11 V/E59 K/E61 T	112.4 ± 0.3	209.6 ± 16.2	3.48 ± 0.02	−39.8 ± 2.1	44.4

*T_d values were determined from the DSC experiments at pH 9.0 and the other values were from the GuHCl denaturation experiments at pH 8.0.
**The difference in $\Delta G^0_{H_2O}$ between the wild-type and mutant.
Positive values of ΔG and $\Delta\Delta G$ mean stabilization. ND means 'not determined'.

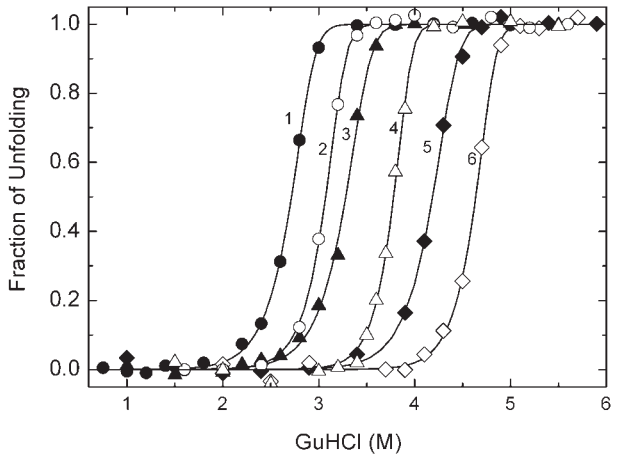

Fig. 3 Typical refolding curves of the wild-type and mutant *Ec*CutA1 at pH 8.0. Numbers 1–6 show the refolding plots of the wild-type, S11 A, E61 V, S11 V/E61 V, S11 V/E61 T/Q73 V and S11 V/E61 V/Q73 V, respectively. These data represent the refolding points of each protein after a 1-day incubation at 37°C as a function of the GuHCl concentration. The solid curves were obtained by fitting of the refolding data to equation (*5*) to obtain the unfolding $\Delta G^0_{H_2O}$ values in Table IV.

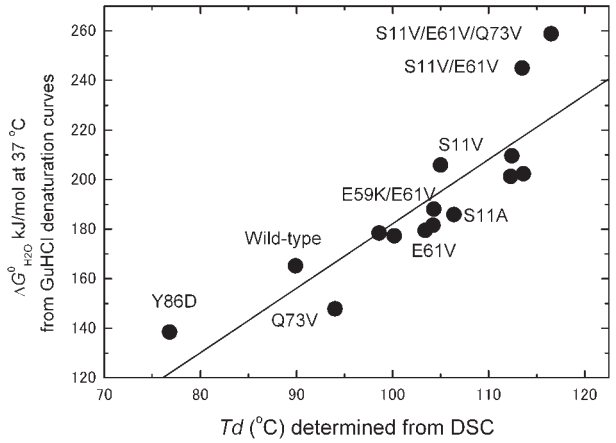

Fig. 4 The relationships between T_d determined from DSC and $\Delta G^0_{H_2O}$ at 37°C from the GuHCl denaturation experiments. All data were obtained from Table IV.

crystal structures of these three mutant proteins were highly similar to the reported wild-type *Ec*CutA1 structure (1NAQ) (*28*). The structures of S11V and S11V/E61V were superimposed with a root mean square deviation (RMSD) of 0.35 ± 0.17 Å between the equivalent Cα atoms from positions 10 to 110 of three subunits in both structures, and the RMSD value between E61V and S11V/E61V was 0.38 ± 0.17 Å. On the other hand, the RMSD values of S11V, E61V, and S11V/E61V versus the wild-type structure (1NAQ) were 0.77 ± 0.40 Å, 0.81 ± 0.41 Å, and 0.80 ± 0.40 Å, respectively. The values among the three mutant proteins were approximately half compared to those between the mutant and wild-type proteins. This difference is due to the high RMSD values of ~4 Å around position 86. In the reported wild-type *Ec*CutA1 structure (*28*), each Cys (3 Cys per subunit) binds a mercury atom or a hydroxyl-mercuribenzoic acid. When the structures of the wild-type protein (1NAQ) and the mutant proteins without mercury are compared, the loop around position 86 of the wild-type protein is pushed out into the solvent, to escape from crushing the mercuribenzoic acids bound to Cys16, resulting in great RMSD values.

Table III shows the SPMP evaluation of three determined structures of *Ec*CutA1 proteins with mutations at positions 11 and 61. The SPMP scores of the mutant

proteins represent average values of each subunit since the *Ec*CutA1 structure consists of three identical subunits. The SPMP values (ΔG_{SPMP}) for S11V at position 11 and E61V at position 61 were remarkably improved from 1.76 to −6.16 kJ/mol and from 0.88 to −2.09 kJ/mol, respectively, and the rank among the 20 amino acid residues increased from 13th to 1st and 12th to 7th, respectively. For the double mutant, the scores at positions 11 and 61 were similar to those of the single mutant protein at each position, indicating that the mutations at each position are independent. The SPMP evaluations suggest that substituting Ser with Val at position 11 improves the stability due to changes in the hydration effect (ΔG_{hyd}), local structure (ΔG_{LC}) and side-chain packing (ΔG_{SP}), whereas substituting Glu with Val at position 61 mainly results in changes in ΔG_{hyd} and ΔG_{LC}. These SPMP evaluations are consistent with the experimental DSC and denaturant denaturation results. The T_d values for S11V and E61V were 105.0 and 103.4°C, respectively, and the T_d value for the double mutant was 113.5°C, suggesting a cumulative effect for each single mutation.

Evaluation of stability changes due to mutations based on tertiary structures

The contribution of some stabilization factors has been quantitatively derived as parameters such as a hydrophobic interaction ($\Delta\Delta G_{HP}$) and hydrogen bond ($\Delta\Delta G_{HB}$) by a unique equation that considers conformational changes due to the mutation(s) using mutant human lysozymes (*4*). The enhanced stabilities of S11V and E61V were expected to improve the local structure based on the SPMP evaluation (Table III), suggesting the conversion to favourable secondary structure. The changes in the propensity to form a secondary structure ($\Delta\Delta G_{pro}$) among the parameters estimated by Funahashi *et al.* (*4*) are useful to elucidate changes in the stability of the two mutants. The $\Delta\Delta G_{pro}$ values of S11V and E61V were calculated to be 1.95 (5.84) and 2.73 kJ/mol (8.18 kJ/mol of a trimer) (Table V), respectively, using the estimated parameter (*4*), suggesting that these mutations improve the protein stability. This occurs because both positions are located in the β-sheet and the two substitutions include residues with a higher propensity to form the β-sheet, which indicates enhanced stabilization. These values are compatible with the experimental results and the SPMP evaluation.

Funahashi *et al.* (*4*) also evaluated the parameters of the hydrophobic interaction. The changes ($\Delta\Delta G_{HP}$) in unfolding Gibbs energy (ΔG) due to mutations, which was caused by hydrophobic interactions, were calculated using equation (*6*) in the 'Experimental procedures' section. Table V shows the energy of the hydrophobic interaction (ΔG_{HP}) at the mutated residues in the three mutant proteins and the difference in ΔG_{HP} due to these mutations ($\Delta\Delta G_{HP}$). For example, the $\Delta\Delta G_{HP}$ value of S11V was calculated to be 8.6 kJ/mol, subtracting the average value (7.3) of ΔG_{HP} at Ser11 in E61V (as the wild-type value) from the average value (15.9) of ΔG_{HP} at Val11 in S11V (Table V). This method was used because ΔG_{HP} at Glu61 of the reported wild-type structure (1NAQ) might be slightly affected by ligands binding to the Cys residues that were previously described, although the average value of ΔG_{HP} at Ser11 in E61V was similar to that of 1NAQ.

These $\Delta\Delta G_{HP}$ values were compared with $\Delta\Delta G^0_{H_2O}$ obtained from the GuHCl denaturation experiments (Table IV). The $\Delta\Delta G^0_{H_2O}$ values for S11V and S11V/E61V, 40.7 and 79.8 kJ/mol, were remarkably larger than the $\Delta\Delta G_{HP}$ values for these two proteins, 25.8 and 54.0 kJ/mol, respectively, suggesting that other factors such as the propensity to form secondary structures contribute to the stabilization of these proteins. In the case of S11V/E61V, the summation of $\Delta\Delta G_{HP}$ and $\Delta\Delta G_{pro}$ was 68.0 kJ/mol and comparable to the $\Delta\Delta G^0_{H_2O}$ value (79.8 kJ/mol), suggesting that the stability of this mutant protein is mainly stabilized by these two factors. On the other hand, the T_d and midpoint of the GuHCl denaturation of E61V are close to those of S11V, but the $\Delta\Delta G^0_{H_2O}$ of E61V was less than half of S11V due to a decrease in the *m* (slope) value (Table IV). It may be necessary to evaluate the changes in the *m* values in more detail.

Table V. Hydrophobic energy of substitution residues of the three mutant proteins evaluated by changes in the *ASA* values and changes in secondary propensity due to mutations.

		ΔG_{HP} (kJ/mol)*					
Proteins	**Position**	**A**	**B**	**C**	**Average values**	**$\Delta\Delta G_{HP}$ (kJ/mol)****	**$\Delta\Delta G_{Pro}$ (kJ/mol)*****
S11 V	Val11	15.9	15.6	16.3	15.9 ± 0.3	8.6(25.8)	2.0(5.9)
	Glu61	8.1	8.8	8.4	8.4 ± 0.2		
E61 V	Ser11	6.8	7.5	7.5	7.3 ± 0.3	8.3(24.9)	2.7(8.2)
	Val61	17.0	16.2	16.9	16.7 ± 0.6		
S11 V/E61 V	Val11	17.5	15.7	15.7	16.3 ± 0.8	18.0(54.0)	4.7(14.0)
	Val61	16.5	17.6	18.0	17.4 ± 0.6		

*A, B and C in a header represent unfolding Gibbs energy of hydrophobic interaction (ΔG_{HP}) at a given residue of each subunit.
**$\Delta\Delta G_{HP}$ represents difference in ΔG_{HP} due to mutations. The values in parentheses represent $\Delta\Delta G_{HP}$ per a trimer.
***Change in propensity to form a secondary structure (ΔG_{Pro}) due to mutations. The values in parentheses represent energies per a trimer. Positive value means stabilization.

Characteristics of stabilized EcCutA1 due to mutations

The tested CutA1 mutants were stabilized at five out of the seven positions that were identified by SPMP. Ser11 in the wild-type protein is almost completely buried in the interior of the molecule and located in the N-terminus of the β-strand. SPMP analysis indicates that the hydration and local structure at Ser11 should be improved (Table II). The 'local structure' score in SPMP evaluates the dihedral angle of each residue in the structure (*19*). In the local structure function of SPMP, the propensity of a single residue to form a favourable secondary structure in the backbone conformation is evaluated by classifying the structure into five states (such as α-helix and β-strand) according to both its position in the $\phi\psi$ space (*i.e.* the Ramachandran plot) (*29*) and the secondary structure based on the definition by Kabsch and Sander (*30*). Therefore, Ser11 was changed to three residues (Val, Ala or Ile) with a higher hydrophobicity and propensity to form a β-sheet. Compared to the wild-type protein, the T_d values of the three mutant proteins, S11A, S11V and S11I, remarkably improved by 16.5, 15.1 and 12.8°C, respectively, and the stabilities against denaturant also increased. Both Val and Ile have a higher hydrophobicity (*31*) and propensity to form a β-sheet (*32*) than Ala. SPMP predicted that S11V has the highest stability among the three mutations (Table II). For S11V, the summation of $\Delta\Delta G$ of the hydrophobicity and the propensity to form a secondary structure based on the structure were also comparable with the experimentally obtained $\Delta\Delta G^0_{H_2O}$ value (Tables IV and V), indicating that drastic changes in the stability due to this mutation are mainly caused by changes in the native structure due to the mutation.

Positions 59, 60 and 61 in a sequential residue number were selected by SPMP to improve the protein stability (Fig. 1). These residues are located in the middle of the β-strand and their side-chains are almost exposed to a solvent. The SPMP scores of Glu59 and Glu61 were reduced due to the penalties associated with local structure, while the score for Tyr60 was reduced due to hydration. The Glu residue at position 59 was substituted with a hydrophobic (Leu), a polar-non-charged (Gln), and an opposite-charged residue (Lys). The T_d values of the three mutants, E59Q, E59L and E59K, improved by 8.4, 10.3 and 14.3°C, respectively, compared to the wild-type protein. The propensity to form a β-sheet is in the order of Leu, Gln, Lys and Glu. The mutant proteins at position 59 might be stabilized by improving the propensity to form a β-sheet, but the T_d of E59K remarkably increased, suggesting that removing the negative charge contributes to the stability of E59L and E59Q. The mutant Y60T, which does not have a penalty for hydration as estimated by SPMP, was stabilized by only 2.0°C. At position 61, Glu was substituted by residues that had the three highest evaluations by SPMP, except for Trp. The T_d values of these three mutants, E61V, E61T and E61H, improved by 13.5, 8.7 and 4.4°C, respectively. The propensity to form a β-sheet was in the order of Val, Thr, His and Glu, which corresponds to the changes in stability. Furthermore, the hydrophobic interaction was estimated to remarkably improve based on the structural changes due to these mutations (Table V). Therefore, in the case of E61V, both the propensity to form a β-sheet and hydration might predominantly contribute to the increased stability. The T_d value of Q73V was increased by 4.1°C. This mutation was expected to reduce the penalty associated with the side-chain packing evaluated by SPMP (Table II).

The stability of the double and triple mutants roughly shows a cumulative effect of each mutant at positions 11, 61 and 73. The T_d of the triple mutant, S11V/E61V/Q73V, was 116.5°C, the highest among the examined mutant proteins, and the ΔT_d between this triple mutant and the wild-type protein was 26.6°C. However, the stabilities of E59K/E61V (104.3°C) and S11V/E59K/E61T (112.4°C) were highly similar to E59K (104.2°C) and S11V/E61T (112.3°C), respectively. In this case, it seems that the stabilization effect of the mutations at position 61 compensates for removing the electrostatic interaction between Lys 59 and Glu61 due to mutations at Glu61, resulting in no cumulative effect on the overall stability. Overall, the drastic increases in stability in the present studies were quantitatively elucidated based on the native structures, although the denatured structures might be affected by the introduced mutations.

Only G45Q and Y86D were remarkably destabilized contrary to the SPMP predictions. Other mutations at these positions were not examined because they are not expected to have greater stability than the wild-type protein.

Conclusions

(i) In order to elucidate the stabilization mechanism of *Ph*CutA1 with a T_d of 150°C, we have tried to improve the heat stability of *Ec*CutA1. First, we chose seven positions in *Ec*CutA1 where the native amino acids were incompatible with the structure according to SPMP.

(ii) The stability of the *Ec*CutA1 mutants for five out of the worst seven positions were remarkably improved compared to the wild-type protein. The highest T_d values for the single (S11A), double (S11V/E61V) and triple (S11V/E61V/Q73V) mutants were 106.4, 113.5 and 116.5°C respectively, at pH 9.0. The T_d values of the double and triple mutants exceeded that for CutA1 from *Thermus thermophilus*. The present results indicate that the stability of *Ec*CutA1 is remarkably improved by a few substitutions, even though the stability of the wild-type protein is unusually high with a T_d of 90°C.

(iii) The heat stabilities (T_d) of the mutant proteins roughly parallel the $\Delta G^0_{H_2O}$ at 37°C that was obtained from GuHCl denaturation. The changes in stability ($\Delta\Delta G^0_{H_2O}$) of the three mutant proteins (S11V, E61V, and S11V/E61V) were drastic, but were quantitatively elucidated based on the newly solved native structure.

(iv) As expected, the SPMP scores at positions 11 and 61 of the mutant structures were improved. The present results confirm that SPMP is a powerful tool to explore amino acid substitutions at specific positions in order to improve the stability of a protein.
(v) The present *Ec*CutA1 mutants with deleted incompatible structures would be good templates to improve the heat stability of *Ec*CutA1 with a T_d (150°C) comparable to that of *Ph*CutA1 with many ionic residues.

Coordinates

Database: structural data are available from the Protein Data Bank under the accession codes for the mutants of *Ec*CutA1, S11V, E61V and S11V/E61V, 3AH6, 3AA9 and 3AA8, respectively.

Acknowledgements

We thank Dr. Yasushi Nitanai (RIKEN SPring-8 Center) for discussions on refinement of the mutant structures. This work was supported in part by a Grant-in-Aid for Scientific Research (C) (No. 20589003 to Y. M. and No. 21570173 and 22570166 to K. Y.) by JSPS of Japan.

Conflict of interest
None declared.

References

1. Pace, C.N., Shirley, B.A., McNutt, M., and Gajiwala, K. (1996) Forces contributing to the conformational stability of proteins. *FASEB J.* **10**, 75–832
2. Privalov, P.L. and Gill, S.J. (1988) Stability of protein structure and hydrophobic interaction. *Adv. Protein Chem.* **39**, 191–234
3. Takano, K., Yamagata, Y., Fujii, S., and Yutani, K. (1997) Contribution of the hydrophobic effect to the stability of human lysozyme: calorimetric studies and X-ray structural analyses of the nine valine to alanine mutants. *Biochemistry* **36**, 688–698
4. Funahashi, J., Takano, K., and Yutani, K. (2001) Are the parameters of various stabilization factors estimated from mutant human lysozymes compatible with other proteins? *Protein Eng.* **14**, 127–134
5. Yutani, K., Ogasahara, K., Sugino, Y., and Matsushiro, A. (1977) Effect of a single amino acid substitution on stability of conformation of a protein. *Nature* **267**, 274–275
6. Alber, T., Dao-pin, S., Wilson, K., Wozniak, J.A., Cook, S.P., and Matthews, B.W. (1987) Contributions of hydrogen bonds of Thr 157 to the thermodynamic stability of phage T4 lysozyme. *Nature* **330**, 41–46
7. Eriksson, A.E., Baase, W.A., Zhang, X.J., Heinz, D.W., Blaber, M., Baldwin, E.P., and Matthews, B.W. (1992) Response of a protein structure to cavity-creating mutations and its relation to the hydrophobic effect. *Science* **255**, 178–183
8. Takano, K., Ogasahara, K., Kaneda, H., Yamagata, Y., Fujii, S., Kanaya, E., Kikuchi, M., Oobatake, M., and Yutani, K. (1995) Contribution of hydrophobic residues to the stability of human lysozyme: calorimetric studies and X-ray structural analysis of the five isoleucine to valine mutants. *J. Mol. Biol.* **254**, 62–76
9. Takano, K., Funahashi, J., Yamagata, Y., Fujii, S., and Yutani, K. (1997) Contribution of water molecules in the interior of a protein to the conformational stability. *J. Mol. Biol.* **274**, 132–142
10. Ogasahara, K., Nakamura, M., Nakura, S., Tsunasawa, S., Kato, I., Yoshimoto, T., and Yutani, K. (1998) The unusual slow unfolding rate causes the high stability of pyrrolidone carboxyl peptidase from a hyperthermophile, *Pyrococcus furiosus*: equilibrium and kinetic studies of guanidine hydrochloride-induced unfolding and refolding. *Biochemistry* **37**, 17537–17544
11. Jaenicke, R. and Bohm, G. (2001) Thermostability of proteins from *Thermotoga maritima*. *Methods Enzymol.* **334**, 458–469
12. Petsko, G.A. (2001) Structural basis of thermostability in hyperthermophilic proteins, or "there's more than one way to skin a cat". *Methods Enzymol.* **334**, 469–478
13. Kaushik, J.K., Ogasahara, K., and Yutani, K. (2002) The unusually slow relaxation kinetics of the folding-unfolding of pyrrolidone carboxyl peptidase from a hyperthermophile, *Pyrococcus furiosus J. Mol. Biol.* **316**, 991–1003
14. Ogasahara, K., Ishida, M., and Yutani, K. (2003) Stimulated interaction between α and β subunits of tryptophan synthase from hyperthermophile enhances its thermal stability. *J. Biol. Chem.* **278**, 8922–8928
15. Tanaka, T., Sawano, M., Ogasahara, K., Sakaguchi, Y., Bagautdinov, B., Katoh, E., Kuroishi, C., Shinkai, A., Yokoyama, S., and Yutani, K. (2006) Hyper-thermostability of CutA1 protein, with a denaturation temperature of nearly 150°C. *FEBS Lett.* **580**, 4224–4230
16. Kirk, O., Borchert, T.V., and Fuglsang, C.C. (2002) Industrial enzyme applications. *Curr. Opin. Biotechnol.* **13**, 345–351
17. Sawano, M., Yamamoto, H., Ogasahara, K., Kidokoro, S., Katoh, S., Ohnuma, T., Katoh, E., Yokoyama, S., and Yutani, K. (2008) Thermodynamic basis for the stabilities of three CutA1s from *Pyrococcus horikoshii, Thermus thermophilus*, and *Oryza sativa*, with unusually high denaturation temperatures. *Biochemistry* **47**, 721–730
18. Ota, M., Kanaya, S., and Nishikawa, K. (1995) Desk-top analysis of the structural stability of various point mutations introduced into ribonuclease H. *J. Mol. Biol.* **248**, 733–738
19. Ota, M. and Nishikawa, K. (1997) Assessment of pseudo-energy potentials by the best-five test: a new use of the three-dimensional profiles of proteins. *Protein Eng.* **10**, 339–351
20. Ota, M., Isogai, Y., and Nishikawa, K. (2001) Knowledge-based potential defined for a rotamer library to design protein sequences. *Protein Eng.* **14**, 557–564
21. Pace, C.N., Vajdos, F., Fee, G., Grimsley, G., and Gray, Y. (1995) How to measure and predict the molar absorption coefficient of a protein. *Protein Sci.* **4**, 2411–2423
22. Backmann, J., Schafer, G., Wyns, L., and Bonisch, H. (1998) Thermodynamics and kinetics of unfolding of the thermostable trimeric adenylate kinase from the archaeon *Sulfolobus acidocaldarius*. *J. Mol. Biol.* **284**, 817–833
23. Vagin, A. and Teplyakov, A. (1997) *MOLREP*: an automated program for molecular replacement. *J. Appl. Cryst.* **30**, 1022–1025
24. Brünger, A.T., Adams, P.D., Clore, G.M., DeLano, W.L., Gros, P., Grosse-Kunstleve, R.W., Jiang, J.S., Kuszewski, J., Nilges, M., Pannu, N.S., Read, R.J., Rice, L.M., Simonson, T., and Warren, G.L. (1998) Crystallography & NMR system: a new software suite

for macromolecular structure determination. *Acta Cryst*. **D54**, 905–921
25. Emsley, P. and Cowton, K. (2004) Coot: model-building tools for molecular graphics. *Acta Cryst*. **D60**, 2126–2132
26. Laskowski, R.A., MacArthur, M.W., Moss, D.S., and Thornton, J.M. (1993) *PROCHECK*: a program to check the stereochemical quality of protein structures. *J. Appl. Cryst*. **26**, 283–291
27. Connolly, M.L. (1993) The molecular surface package. *J. Mol. Graphics* **11**, 139–141
28. Arnesano, F., Banci, L., Benvenuti, M., Bertini, I., Calderone, V., Mangani, S., and Viezzoli, M.S. (2003) The evolutionarily conserved trimeric structure of CutA1 proteins suggests a role in signal transduction. *J. Biol. Chem*. **278**, 45999–46006
29. Nishikawa, K. and Matsuo, Y. (1993) Development of pseudoenergy potentials for assessing protein 3-D-1-D compatibility and detecting weak homologies. *Protein Eng*. **6**, 811–820
30. Kabsch, W. and Sander, C. (1983) Dictionary of protein secondary structure: pattern recognition of hydrogen-bonded and geometrical features. *Biopolymers* **22**, 2577–2637
31. Kyte, J. and Doolittle, R F. (1982) A simple method for displaying the hydropathic character of a protein. *J. Mol. Biol*. **157**, 105–132
32. Chou, P.Y. and Fasman, G.D. (1978) Prediction of the secondary structure of proteins from their amino acid sequence. *Adv. Enzymol*. **47**, 45–148